Available online at www.sciencedirect.com
SCIENCE DIRECT®
Computers and Electronics in Agriculture 47 (2005) 59–67
Computers and electronics in agriculture
www.elsevier.com/locate/compag

Application note

A MATLAB graphical user interface program for tomographic viscometer data processing

Young Jin Choi, Kathryn L. McCarthy, Michael J. McCarthy*

Department of Food Science and Technology, University of California, Davis, CA 95616, USA

Received 4 August 2003; received in revised form 17 May 2004; accepted 10 August 2004

Abstract

A MATLAB-based graphical user interface (GUI) program has been developed and implemented for tomographic viscometer data processing. The tomographic viscometer is based on a velocity profile measurement using magnetic resonance imaging (MRI) or ultrasonic Doppler velocimetry (UDV). The main data processing includes the velocity image reconstruction, velocity profile generation, velocity profile curve fitting, rheograms construction and constitutive model fitting. This program enables users to process image data, to calculate rheological properties and to visualize results. The program code consists of a set of files, which can be modified to match other purposes as well. This program may also serve as a tool for real-time monitoring and process control.

Keywords: MATLAB; Tomographic viscometer; Graphical user interface (GUI)

1. Introduction

In the food and agricultural industries, many processes utilize materials which have complex rheological properties. Since the rheological properties, such as shear viscosity, slip velocity and yield stress, govern the performance of unit operations, it is useful to monitor the rheological properties for process control and product quality assurance. Most process measurements of viscosity are single shear rate measurements (Cullen et al., 2000). Recently,

* Corresponding author. Tel.: +1 530 752 8921; fax: +1 530 752 4759.
E-mail address: mjmccarthy@ucdavis.edu (M.J. McCarthy).

doi:10.1016/j.compag.2004.08.001

multi-shear rate measurements of rheological properties have been developed based on tomographic methods. Tomography is a technique for obtaining two-dimensional images from three-dimensional objects (Scott, 1995) and has been widely used in medical diagnostic tools. The potential of tomographic techniques was well recognized early in the 1950s and a variety of applications have been applied to industrial processes since (Beck and Williams, 1996; Beck et al., 1998). Non-invasive and -destructive measurement characteristics of the tomographic techniques are suitable for measuring the material distribution and velocity profile within a pipe in real-time (Williams and Beck, 1995). In-line tomographic pipe viscometers have been developed that are suitable for process environments (Arola et al., 1997a,b; Sadkin, 1999; Cullen et al., 2000; Choi, 2003).

Analysis of tomographic data generally includes signal processing, image processing, and graphical display. MATLAB-based software for analysis of tomographic data has been developed for a wide range of applications (Harley and Loftus, 2000). These applications include processing and simulation of geophysical data (Whitten, 2002), analysis of microarray in mRNA levels of genes (Venet, 2003), bioprocess simulation (Sevella and Bertalan, 2000) and analysis of neuronal activity (Egert et al., 2002). These types of programs serve as both research tools and educational tools. Characterization of product physical properties such as rheology, moisture content and degree of mixing using tomographic data requires the development of efficient data processing methods.

This paper presents a MATLAB-based software program for analysis of fluid rheological properties. The data are acquired utilizing tomography. The tomographic techniques magnetic resonance imaging (MRI) and ultrasonic Doppler velocimetry (UDV) are used to measure fluid velocity as a function of radial position for material undergoing steady pressure driven pipe flow. Through a series of processing steps based on a graphical user interface (GUI), these data are converted to a rheogram for the fluid. It is assumed that the reader is familiar with fluid rheology. A good basic reference for agricultural products is Steffe (1996).

2. Program structure

The GUI data processing program allows a user to process tomographic data from either MRI or UDV and to calculate rheological properties immediately after data acquisition. The program is a set of m-files and consists of four major parts (an m-file is a user-defined function or script file composed of existing MATLAB commands and functions): reconstruction of velocity profile image, generation of the velocity profile, determination of shear rate, and application of constitutive models. The structure of the program is shown in Fig. 1.

2.1. Reconstruction of velocity profile image

Starting the GUI program is initiated in the command window of MATLAB with the ‘viscometer’ command. Invoking the GUI program command opens a window where the user is prompted to select the data type. Selecting the data type opens a corresponding window for selection of the data and reading of the time-domain tomographic data. The experimental parameters are categorized as the flow loop parameters and tomographic parameters (MRI or UDV parameters).

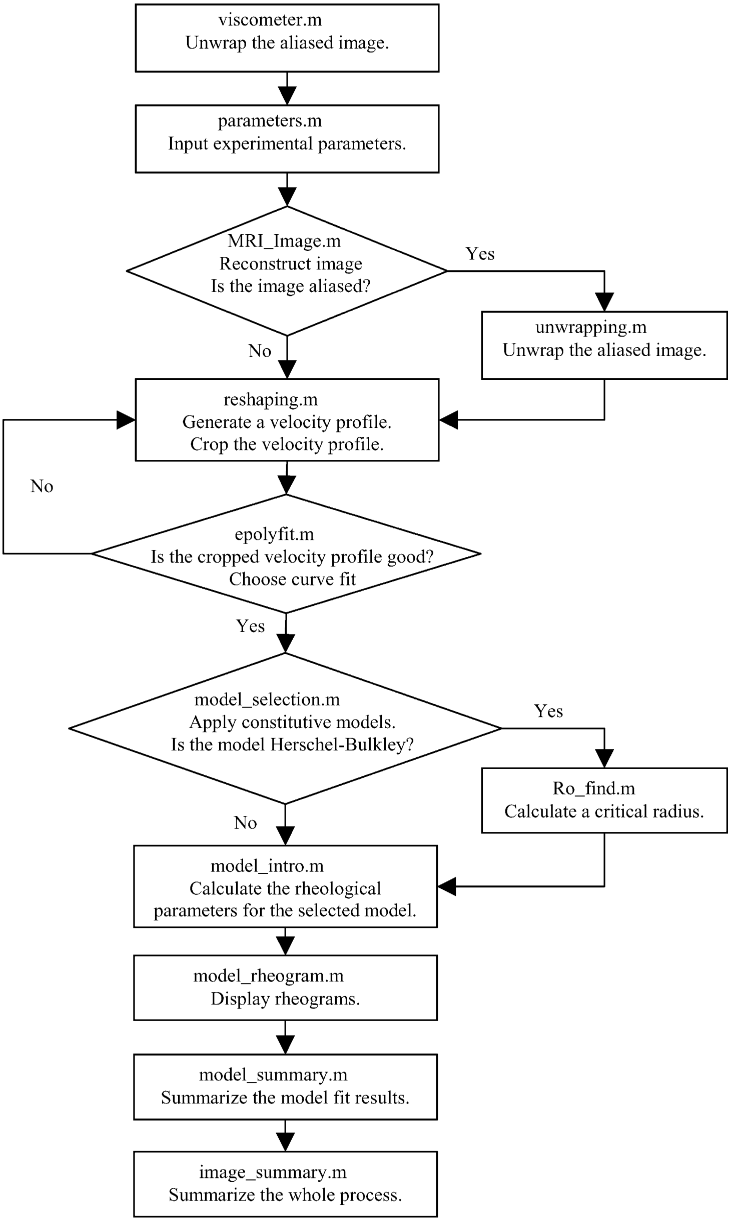

Fig. 1. Flowchart for tomographic viscometer data processing program.

Data from both MRI and UDV are acquired in the time domain. The MRI data matrix consists of complex pairs for each data acquisition. The size of rows and columns in the matrix correspond to the number of phase encoding steps and the number of frequency encoding steps. Prior to image reconstruction, filtering and zero-filling may be applied to the data matrix. Filtering improves the signal-to-noise ratio by removing high frequency noise and zero-filling improves the resolution of the image. The processed data matrix is then Fourier transformed and the magnitude image is used for determining the velocity profile.

The UDV time-domain data matrix is a set of multiple echoes. Each row represents one echo signal so that the number of rows equals the number of pulse repetitions and the number of columns is the number of samples across the pipe. After zeroing any dc component, Fourier transformation is applied to each radial distance yielding instantaneous Doppler shifted frequencies, which are a function of the fluid velocity at that radial distance (Takeda, 1991).

If the velocity profile image is aliased, unwrapping the image is necessary prior to further image processing. Sampling below the Nyquist frequency results in an aliased velocity profile. As long as the aliasing is not so extreme that the velocity profile ridge overlaps itself, the true high resolution velocity profile can be extracted from the aliased velocity data (Arola et al., 1997a,b).

2.2. Generation of velocity profile

The second data processing step is to extract the velocity profile from the velocity image. The image is thresholded to remove noise and the remaining signal values are averaged to yield the velocity profile. In the velocity direction, the zero velocity position is determined from an image taken under a no flow condition. The radial limit depends on the field of view setting that determines the number of pixels across the pipe diameter. Generally, the velocity profile begins at the zero velocity position next to the wall (i.e., no slip condition at pipe wall). However, by knowing the zero velocity position and radial limits, slip velocity may also be determined directly from an image (Gibbs et al., 1996).

The MRI velocity profile points are converted from pixels to actual dimensions using the velocity sweep width (vsw), field of view (fov) and pipe radius (r). The increment in the velocity direction ($\mathrm{d}v$) is:

$$\mathrm{d}v = \frac{\mathrm{vsw}}{n_v} \tag{1}$$

where n_v is total number of pixels in velocity direction. The increment in the radial direction ($\mathrm{d}r$) is:

$$\mathrm{d}r = \frac{\mathrm{fov}}{n_r} \tag{2}$$

where n_r is total number of pixels in radial direction.

For UDV data, the increment in the velocity direction is a function of the number of pulse repetition, f_r; speed of ultrasound, v_c; basic ultrasound frequency, f_0; the angle inclination, θ of the transducer; and the number of echo acquisitions, n_x. The increment in the velocity direction is:

$$\mathrm{d}v = \frac{v_c f_r}{2 f_0 \cos\theta n_x} \tag{3}$$

The increment in the radial direction is dependent on the sampling frequency, f_s; ultrasound speed; and angle of inclination through:

$$dr = \frac{v_c}{2 f_s} \cos\theta \tag{4}$$

2.3. Shear rate determination

Curve fitting of the velocity profile is used to determine shear rate values. The method involves using a polynomial function as a global curve fit to the velocity profile data points (Arola et al., 1997b). The polynomial is differentiated to yield the shear rate at each radial position in the velocity profile. Before fitting a constitutive model, the apparent shear viscosity η is calculated using the following equation:

$$\eta(r) = \frac{\sigma(r)}{\dot{\gamma}(r)} \tag{5}$$

where σ is shear stress and $\dot{\gamma}$ is shear rate. A low degree even order polynomial is sufficient for fitting a parabolic velocity profile of a Newtonian or power law fluid. However, a higher degree polynomial is often needed to fit the velocity profile characteristic of a Bingham plastic, Casson or Herschel–Bulkley fluid.

2.4. Application of a constitutive model

Prior to fitting the data with rheological models, maximum and minimum shear rate values are specified. Default options are a minimum shear rate at $0.01r$ and a maximum shear rate at $0.825r$. These values are used as a guideline to minimize the errors resulting from the curve fit to the velocity profile at the pipe center (low shear rate region) and near the wall (high shear rate region). Uncertainty becomes large in the low shear rate region because the velocity resolution is the same order of magnitude as the shear rate that is being approximated. Errors at the wall result from partial volume effects and low signal in the high shear rate region.

The velocity profile can be modeled with common constitutive models: Newtonian, power law, Bingham plastic, Casson and Herschel–Bulkley. Selecting a model from the menu links to a corresponding window which provides rheograms of shear rate against radius, shear stress versus shear rate (Fig. 2a), shear viscosity versus shear rate, and a model curve fit of the velocity profile (Fig. 2b).

The models, except the Casson model, are generalized with the Herschel–Bulkley model which has three parameters: yield stress, σ_0; consistency index, K; and flow behavior index, n. For the Herschel–Bulkley model, the velocity profile normalized by the maximum velocity is given by:

$$\begin{aligned} \frac{v}{v_{\max}} &= 1 - \left(\frac{c - c_0}{1 - c_0}\right)^{(n+1)/n}; \quad && c_0 \le c \le 1 \\ \frac{v}{v_{\max}} &= 1; && c \le c_0 \end{aligned} \tag{6}$$

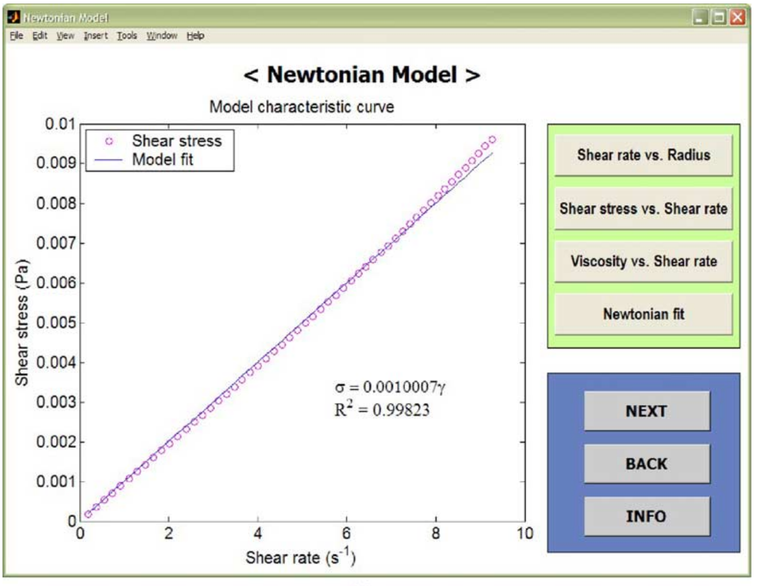

(a)

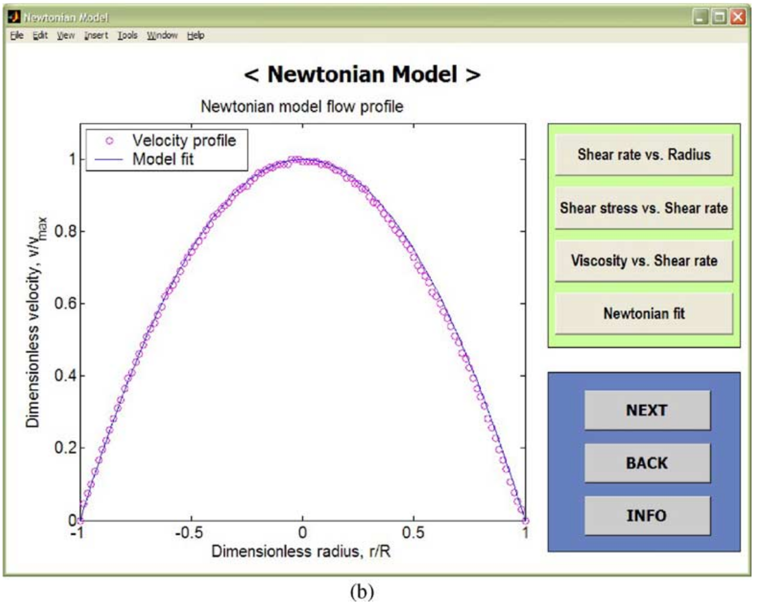

(b)

Fig. 2. GUI for displaying rheograms: (a) shear rate vs. shear stress and (d) model curve fit plots.

where c is r/R; r, the radial position; R, the pipe radius; and r_0, the critical radius defined as $r_0 = (2\sigma_0 L)/\Delta P$, where $\rho P/L$ is the pressure drop over a known pipe length. The parameter c_0 is the dimensionless critical radius given by r_0/R. The first order derivative of Eq. (6) with respect to c yields the dimensionless shear rate:

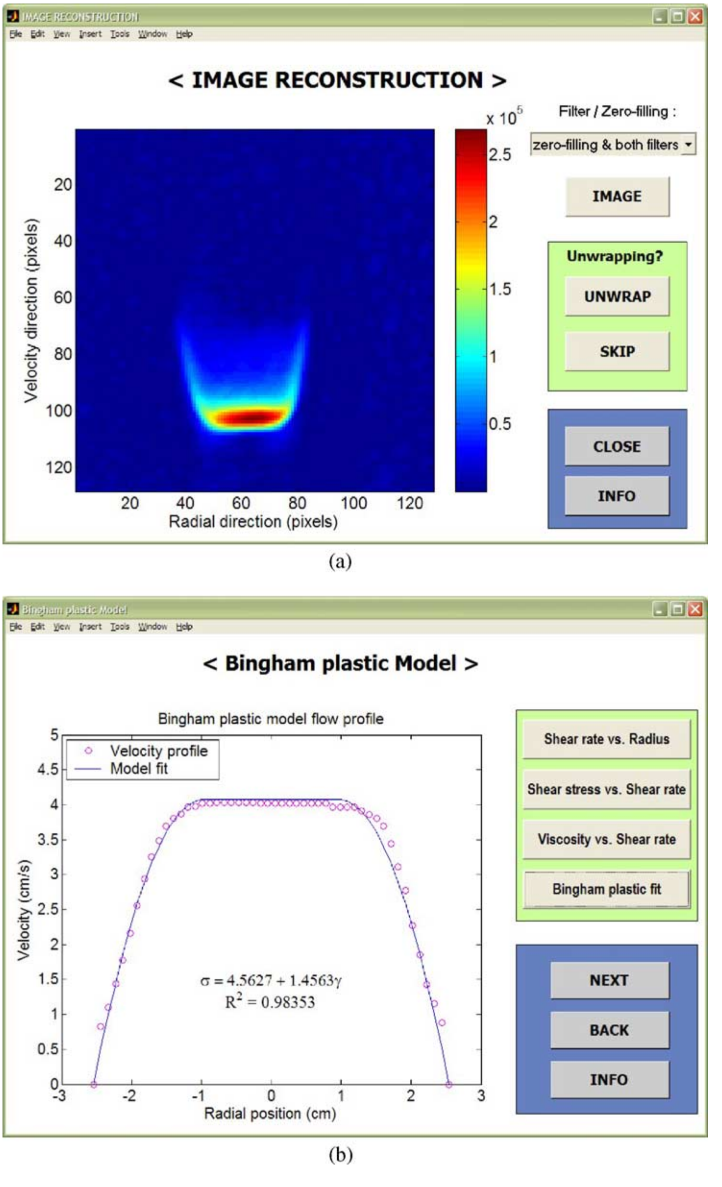

Fig. 3. Application of the models for tomato juice flow: (a) velocity image and (b) Bingham plastic model fit to velocity profile.

$$\dot{\gamma}_1 = \left(\frac{n+1}{n}\right)\left(\frac{c-c_0}{1-c_0}\right)^{1/n}\left(\frac{1}{1-c}\right); \quad c_0 \le c \le 1 \tag{7}$$

where the subscript 1 denotes a dimensionless quantity. Then, the relationship between dimensionless radius and dimensionless shear rates is given by:

$$c - c_0 = K_1 \dot{\gamma}_1^n \tag{8}$$

where $K_1 = K(2L/R\Delta P)(v_{max}/R)^n$.

For a Newtonian fluid, the flow behavior index n and dimensionless critical radius c_0 in Eq. (8) are 1 and 0, respectively. After plotting c versus $\dot{\gamma}_1^n$, K_1 is determined from the slope of the linear regression. For a power law fluid, which has no yield stress (i.e., $c_0 = 0$), a plot of $\log c$ versus $\log \dot{\gamma}_1$ yields a slope n, and an intercept $\log K_1$. When n is 1, Eq. (8) reduces to a Bingham plastic model. A plot of c versus $\dot{\gamma}_1$ provides a slope K_1 and an intercept c_0. Since the Herschel–Bulkley model has three unknown parameters to be determined, an iteration scheme is utilized. First, the critical radius is estimated from the velocity profile. Then, the flow behavior index n and consistency index K_1 are estimated from the slope and intercept, respectively, of the plot of $\log(c - c_0)$ versus $\log \dot{\gamma}_1$. If c_0 was an accurate estimation, the plot of c versus $K_1\dot{\gamma}_1^n$ yields a slope of 1 and an intercept equal to c_0. Otherwise, a new c_0 is estimated and the procedure repeated until the absolute value of (slope − 1) is within the precision limits. For the Casson model, a plot of $\sigma^{0.5}$ versus $\dot{\gamma}^{0.5}$ yields a slope, which is the Casson plastic viscosity and an intercept of $\sigma_0^{0.5}$.

3. Application example

Characterization of the rheological properties of tomato-based suspension is useful for process design, quality assurance and process control. An MR image of a tomato juice (4.2° brix) at a flow rate of 56 ml/s is shown in Fig. 3a. The flow profile has plug flow region at the pipe center, which is typical for suspension flows. In general, as the flow rate increases, the plug flow region decreases. Fig. 3b shows the best fit rheological model for this fluid which is the Bingham plastic model. These results can be utilized to estimate quality assurance parameters for this product (McCarthy and McCarthy, 1997).

In summary, the MATLAB-based GUI program for a tomographic viscometer has been developed and implemented successfully. This program provides a rapid method to process data and obtain rheological information. This program is also useful for real-time monitoring and control of fluid processing operations.

References

Arola, D.F., Barrall, G.A., Powell, R.L., McCarthy, K.L., McCarthy, M.J., 1997a. Use of nuclear magnetic imaging as a viscometer for process monitoring. Chem. Eng. Sci. 52 (13), 2049–2057.

Arola, D.F., Barrall, G.A., Powell, R.L., McCarthy, M.J., 1997b. Measurement time reducing methods for NMR flow profile imaging: Hankel transforms, velocity aliasing and rapid repetition time. J. Magn. Reson. Anal. 7, 175–184.

Beck, M.S., Williams, R.A., 1996. Process tomography: a European innovation and its applications. Meas. Sci. Technol. 7 (3), 215–224.

Beck, M.S., Dyakowski, T., Williams, R.A., 1998. Process tomography-the state of the art. Trans. Inst. Meas. Control 20 (4), 163–177.

Choi, Y.J., 2003. Application of tomographic techniques for rheological measurements and process control. Ph.D. dissertation. University of California, Davis, California.

Cullen, P.J., Duffy, A.P., O'Donnell, C.P., O'Callaghan, D.J., 2000. Process viscometry for the food industry. Trends Food Sci. Technol. 11, 451–457.

Egert, U., Knott, Th., Schwartz, C., Nawrot, M., Brandt, A., Rotter, S., Diesmann, M., 2002. AEA-tools: an open source toolbox for the analysis of multi-electrode data with MATLAB. J. Neurosci. Methods 117 (1), 33–42.

Gibbs, S.J., James, K.L., Hall, L.D., 1996. Rheometry and detection of apparent wall slip for Poiseuille flow of polymer solutions and particulate dispersions by nuclear magnetic resonance velocimetry. J. Rheol. 40 (3), 425–440.

Harley, E.M., Loftus, G.R., 2000. MATLAB and graphical user interfaces: tools for experiment management. Behav. Res. Methods Instrum. Comput. 32 (2), 290–296.

McCarthy, M.J., McCarthy, K.L., 1997. Food quality prediction from process tomography and flow modeling. In: Windhab, E.J., Wolf, B. (Eds.), Food Rheology and Structure. I. Proceedings of the 1st International Symposium on Food Rheology and Structure. Zurich, Switzerland, pp. 76–78.

Sadkin, S., 1999. Viscometric measurement by nuclear magnetic resonance imaging. M.S. dissertation. University of California, Davis, California.

Scott, D.M. (Ed.), 1995. Frontiers in Industrial Process Tomography. Engineering Foundation, New York.

Sevella, B., Bertalan, G., 2000. Development of a MATLAB based bioprocess simulation tool. Bioprocess. Eng. 23, 621–626.

Steffe, J.F., 1996. Rheological Methods in Food Process Engineering, second ed. Freeman Press, East Lansing, MI.

Takeda, Y., 1991. Development of an ultrasound velocity profile monitor. Nucl. Eng. Design 126 (2), 277–284.

Venet, D., 2003. MatArray: a MATLAB toolbox for microarray data. Bioinformatics 19 (5), 659–660.

Whitten, A., 2002. Geophysica: MATLAB-based software for the simulation, display and processing of nea-surface geophysical data. Comput. Geosci. 28, 751–762.

Williams, R.A., Beck, M.S., 1995. Process Tomography—Principles Techniques and Applications. Butterworth-Heinemann, London.